

NASA TM- 77106

NASA TECHNICAL MEMORANDUM NASA-TM-77106 19830021902

NASA TM- 77106

PHOTOIONIZATION RESEARCH ON ATOMIC BEAMS. II.

The Photoionization Cross Section of Atomic Oxygen

F. J. Comes, F. Speier and A. Elzer

Translation of "Photoionizationsuntersuchungen an Atomstrahlen. II.,  
Der Ionisierungsquerschnitt des atomaren Sauerstoffs," Zeitschrift  
fuer Naturforschung, Ausgabe A, Vol. 23A, No. 1, January 1968,  
pp. 125-133.

LIBRARY COPY

JAN 27 1984

LANGLEY RESEARCH CENTER  
LIBRARY, NASA  
HAMPTON, VIRGINIA

NATIONAL AERONAUTICS AND SPACE ADMINISTRATION  
WASHINGTON, D.C. 20546

AUGUST 1982



NF00307

1. Report No. NASA TM-77106		2. Government Accession No.		3. Report's Catalog No.	
4. Title and Subtitle PHOTOIONIZATION RESEARCH ON ATOMIC BEAMS. II. The Photoionization Cross Section of Atomic Oxygen				5. Report Date August 8, 1982	
7. Author(s) F. J. Comes, F. Speier, and A. Elzer Physical Chemistry Institute, Bonn University				6. Performing Organization Code	
8. Performing Organization Name and Address Leo Kanner Associates, P.O. Box 5187 Redwood City, California 94063				9. Performing Organization Report No.	
12. Sponsoring Agency Name and Address National Aeronautics and Space Adminis- tration, Washington, D.C. 20546				10. Work Unit No.	
11. Contract or Grant No. NASw-3541				13. Type of Report and Period Covered Translation	
14. Sponsoring Agency Code					
15. Supplementary Notes Translation of "Photoionizationsuntersuchungen an Atom- strahlen. II., Der Ionisierungsquerschnitt des atomaren Sauerstoffs," Zeitschrift fuer Naturforschung, Ausgabe A, Vol. 23A, No. 1, Jan- uary 1968, pp. 125-133. (A68-20280)					
16. Abstract An experiment to determine the absolute value of the photo- ionization cross section of atomic oxygen is described. The atoms are produced in an electrical discharge in oxygen gas with 1% hydrogen added. In order to prevent recombination a crossed beam technique is employed. The ions formed are detected by a time-of-flight mass spectrometer. The concen- tration of oxygen atoms in the beam is 57%. The measured photoionization cross section of atomic oxy- gen is compared with theoretical data. The results show the participation of autoionization processes in ionization. The cross section at the autoionizing levels detected is considerably higher than the absorption due to the unper- turbed continuum. Except for wavelengths where autoioniz- ation occurs, the measured ionization cross section is in fair agreement with theory. This holds up to 550 A wheras for shorter wavelengths the theoretical values are much high- er.					
17. Key Words (Selected by Author(s))			18. Distribution Statement Unclassified-Unlimited		
19. Security Class. of this report Unclassified		20. Security Class. of this page Unclassified		21. No. of Pages 22	

PHOTOIONIZATION RESEARCH ON ATOMIC BEAMS. II.

The Photoionization Cross Section of Atomic Oxygen

F.J. Comes, F. Speier, and A. Elzer

Physical Chemistry Institute, Bonn University

In two previous papers, a method to determine photoelectrical yields absolutely was described [1,2]. The process employs the photoionization of an atomic hydrogen beam that passes through the ion source of a suitable mass spectrometer. Since the effective cross section of the hydrogen atom can be calculated exactly, an absolute photon count can be undertaken with the measured proton beam. An oxygen atom beam was generated in the same atomic beam generator apparatus, and the photoionization cross section was measured.

In molecular and atomic form, oxygen is a major component of the earth's atmosphere. Whereas oxygen at low elevations appears only in molecular form, in the medium or high reaches of the ionosphere it primarily, and sometimes exclusively, exists in atomic form. Atomic oxygen is the most frequently found gas above 200 km. Not until an altitude of 500 km is reached does it lose this distinction to helium, and later, to atomic nitrogen.

Degree of ionization is determined through particle density and two other factors: spectral distribution of primary radiation and the energy declivity of the ionization cross section. The spectrum of sunlight that penetrates the ionosphere was measured in a series of satellite passes, as well as by high-altitude research rockets. The effective cross section of the oxygen atom was calculated by several authors.<sup>3,4,5</sup> There are considerable deviations between the individual calculations. Measurement of the photoionization of the oxygen atom has until now not been undertaken. However, just an absorption measurement in "active" oxygen with a line spectrum background was undertaken.<sup>6</sup> An oxygen-helium mixture gas resultant to a microwave discharge passed through an absorption chamber, and the measured range lay between 900 and 500 A.

### Experimental

The apparatus (Fig. 1) has already been described thoroughly.<sup>2</sup> It consists of a UV monochromator in Seya layout, a mass spectrometer, and an atomic beam circuit. The light source was a capillary spark gap. The bandwidth of the light beam at the exit aperture of the monochromator was 2.5 A. Ions were detected by a time-of-flight mass spectrometer. Oxygen dissociation was undertaken in an electrical discharge. To measure the oxygen effective cross section, absolute calibration of a gold photocathode by the hydrogen atomic beam method was accomplished; its photoelectric yield is shown in Fig. 2.

There were 1% H<sub>2</sub> and 8% Argon were added to the entered oxygen. The maximum attained concentration of oxygen atoms in the beam was 57%. Two mass spectra of oxygen are shown in Fig. 3. Fig. 3.A. represents a spectrum without discharge and a wavelength of 610 A. There is sufficient UV radiation energy to generate dissociative ionization of the

oxygen molecule. The second depiction (Fig. 3.B.) shows a spectrum resultant to 670 A wavelength light during continuing discharge, e.g. continuing oxygen production. Since the energy does not suffice to build  $\text{OH}^+$ , only the ion peaks of the oxygen atom and the water molecule below mass 20 are discernable.

Because of intensity requirements, the light source utilized was a capillary spark gap. Under certain experimental conditions, such a light source emanates an intense line spectrum. In the wavelength range from 910 A (the ionization potential of the oxygen atom) and 449 A, 35 lines could be used to measure the oxygen cross section. Since line spacing was almost equidistant throughout the entire spectrum, this signifies that about one line per 14 A was available for measuring purposes. The individual lines of the light source spectrum were not always completely resolveable. One can, however, obtain an overview about the individual lines through spectral tables, since it is known that the majority of the emission lines are oxygen-, nitrogen-, and argon lines.

Figure One: Schematic Drawing of Beam Arrangement

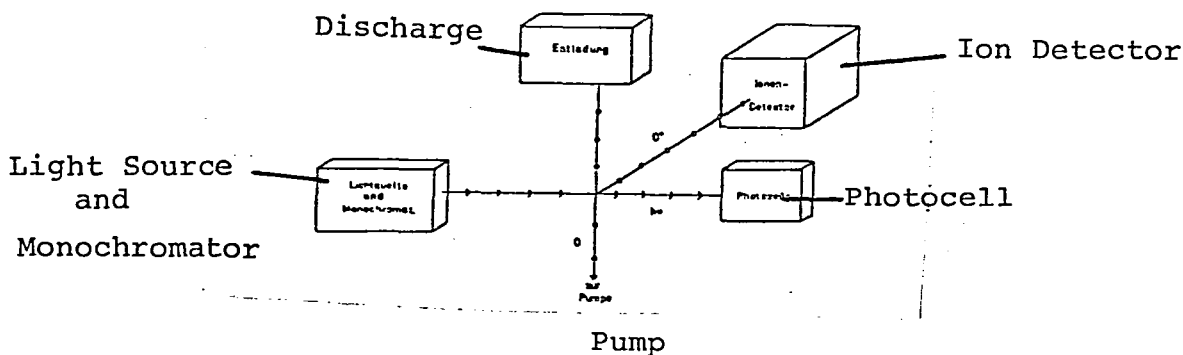


Figure 2. Photoelectric Yield of Gold Cathode

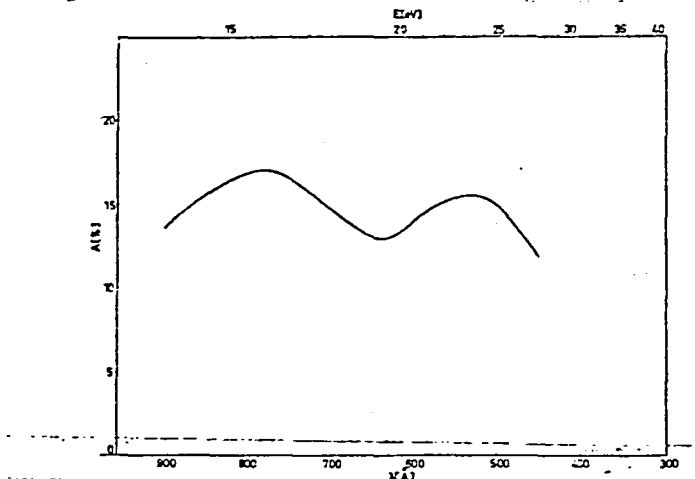
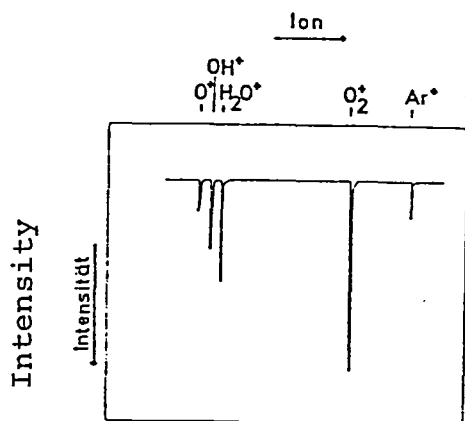
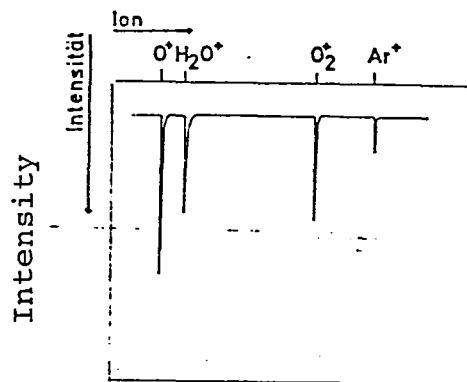


Figure 3.A.



Mass spectrum for the irradiated wavelength 610 Å without discharge. O<sup>+</sup> results only from dissociative ionization.

Figure 3.B.



Mass spectrum for the irradiated wavelength 670 Å with discharge. O<sup>+</sup> results only from photoionization of the oxygen atom.

## Conducting the Measurements and Results Thereto

Measuring the O-ionization cross section is formally composed of two parts: 1. Measuring the effective cross section as a function of the wavelength of light in relative units, and 2. measuring the effective cross section in absolute units at a wavelength  $\lambda_0$ . Two workable methods exist for the second step. First, the absolute effective cross section can be derived from a pure  $O^+$  measurement. The effective cross section  $\sigma(O^+, 0)$  for the photoionization of the oxygen atom as a function of wavelength  $\lambda$  is then expressed as

$$\sigma(O^+, 0) = \frac{I(O^+) A(\lambda)}{I_{phe} V_m T_m A_m Z g t} \quad (1)$$

where:

- $A(\lambda)$  is the photoelectric yield of the gold cathode at wavelength  $\lambda$ ,  
 $I_{phe}$  is the photoelectron current,  
 $I(O^+)$  is the multiplier signal of the  $O^+$  ion current,  
 $V_m$  is the amplification factor of the multiplier,  
 $T_m$  is the mass spectrometer transmission for  $O^+$  ions,  
 $A_m$  is the secondary electron yield of the multiplier cathode for  $O^+$  ions,  
 $Z$  is the number of O-atoms per second that leave the exit aperture of the atomic beam generator (circuit),  
 $t$  is the average volume particle transit time in atom and photon beam,  
 $g$  is the geometry factor

In order to determine the absolute effective cross section according to (1), in addition to the measured currents  $I(O^+)$ ,  $I_{phe}$ , and the yield  $A(\lambda)$ , the values of  $V_m$ ,  $T_m$ ,  $A_m$ ,  $Z$ ,  $g$ , and  $t$  must be known. Because of the low  $O^+$  ion currents, such a measurement is quite difficult.

One can, however, utilize a second procedure of absolute measurement that leads to a much more exact value of  $\sigma(O^+, O)$ , and was employed here. First, the ion source of the mass spectrometer was replaced by an ion chamber<sup>2</sup>, and the ion current formed in  $O_2, I(O_2^+)$  for a suitable wavelength  $\lambda_0$  was determined. (Known geometry circuit). Since the yield of the photocathode is known, we obtain the  $O_2^+$ -production effective cross section  $\sigma(O_2^+, O_2)$  resultant to one pressure- and two current measurements. The ion current provides the ion/second count through utilization of a suitable electrometer amplifier. If one establishes an equation for  $\sigma(O_2^+, O_2)$  that corresponds to equation (1), one is able to establish relationship (2) for the same wavelength  $\lambda_0$ .

$$\sigma(O^+, O) = \sigma(O_2^+, O_2) \frac{I(O^+) A_m(O_2^+)}{I(O_2^+) A_m(O^+)} \cdot \frac{1-\alpha}{\alpha} \quad (2)$$

Additionally, to measure  $\sigma(O^+, O)$  for a particular atom concentration  $\alpha$  with a mass spectrometer, the ion current relationship  $I(O^+)/I(O_2^+)$  as well as the relationship of the secondary electron yields  $A_m(O_2^+)/A_m(O^+)$  for  $O_2^+$  and  $O^+$  ions must be determined. The latter occurs through the recording of an impulse peak spectrum at the multiplier exit for both ion types  $O_2^+$  and  $O^+$ . The relationship is the result of the middle impulse peaks of the Poisson distributions resultant to both. Therewith, the ionization cross section of the oxygen atom for a fixed wavelength  $\lambda_0$  is absolutely determined. By adjusting the relative values at this point the absolute effective cross section for the entire wavelength range can be determined. To carry out these measurements, the oxygen atoms were produced in a direct current discharge in oxygen with hydrogen and argon additives. Oxygen dissociation in a electrical discharge has many advantages over the thermal decay process with regards

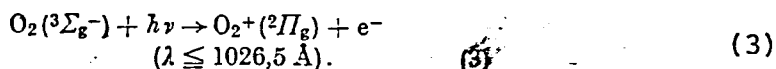


to the experiment to be carried out. As KAUFMAN and KELSO<sup>7</sup> noted, limited hydrogen additives suffice to heighten the degree of dissociation radically. A similar, but lesser influence was noticed by these authors with the addition of  $N_2O$ ,  $N_2$ , and  $NO$ . In contrast,  $He$ ,  $CO_2$  and  $Ar$  did not influence the dissociation. For this reason we chose an admixture of 1%  $H_2$  gas. The admixture of 8% argon served to measure the temperature of the particles in the atom beam. The temperature was  $100 \pm 25^\circ C$ .

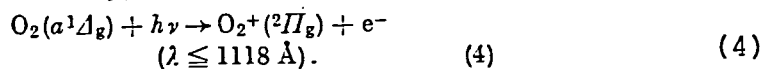
Measuring the degree of dissociation, i.e. the atom concentration  $\alpha$ , was accomplished exclusively through  $O_2^+$  determination. Additionally, the ion beam of the molecular ions with and without discharge was determined. When considering the warming caused by the discharge, this relationship is a direct measure of the dissociation. Ions, electrons, and neutral particles, however, do not have a uniform temperature. In this apparatus, however, the formed oxygen atoms must pass a buffer volume, in which they experience a number of wall collisions and gas shocks, before they reach the aperture of the atom beam generator (circuit). These collisions lead to a far-reaching thermalization of the particles and the deactivation of excited states. One can, therefore, in a good approximation, determine the change in density in the atom beam from the change in intensity of the argon ions resultant to higher temperature.

A knowledge of the componental makeup of the atom beam is necessary to measure the  $O^+$  formation from oxygen atoms in the electronic basic state. From the calculation of other authors we know that the discharge contains metastable oxygen atoms as well as molecules. Since metastable molecules can be ionized throughout the entire measurement spectrum ( $\lambda \leq 910 \text{ \AA}$ ) due to their low ionization energy, their portion of

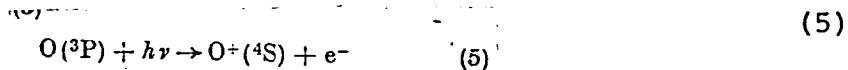
the total ion formation can be determined in advance. Primarily  $O_2$  molecules in the  $a^1\Delta_g$  state and with lesser concentration in the  $b^1\Sigma_g^+$  state are noted as metastable molecules in oxygen discharges.<sup>8</sup> Oxygen atom metastable states are the  $^1D$  and the  $^1S$  states. The presence of metastable excited particles in the beam is quite precisely determinable through the photoionization method. The wavelength 1026.5 Å corresponds to the ionization potential of the oxygen molecule.



$O_2$  molecules in the lowest metastable state have an ionization potential about 1 eV lower.

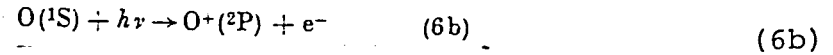
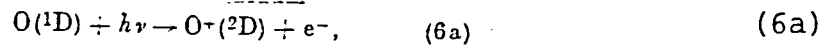


Ion formation at 1086 Å was tested to check for the presence of metastable molecular states. No  $O_2$  ions were found. Since the ionization cross sections of metastable oxygen molecules are not known, one can not determine the upper limit of metastable particle density from the sensitivity of the measuring apparatus. One can, however, determine the maximal portion of metastable molecules in the measured  $O_2^+$  beam, which, according to Equation (5), is singularly significant for the measurement of ionization probability. This portion is less than 3% of the ions in the basic state.



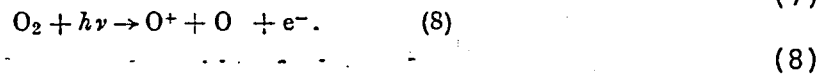
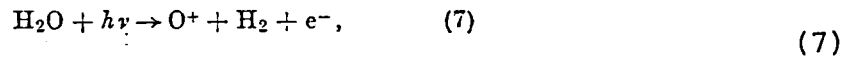
The O-atoms metastable states are the  $^1D$  and the  $^1S$  states. The transitions into the ion basic state are optically impossible from these states. The lowest ionization potential for such a transition from these

metastable atomic states into the ionization continuum

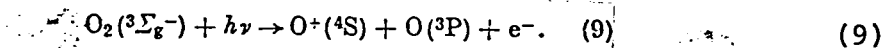


correspond to the wavelengths 828.0 and 858.3 Å. Both ionization potentials lie in the continuum of not excited atoms. The deactivation of  $O(^1D)$  and also  $O(^1S)$  in a collision with  $O_2$  molecules is so fast,<sup>9</sup> that a disappearing probability of existence of metastable atoms in the beam manifests itself. These conclusions correspond to electron collision experiments quite well<sup>8, 10.</sup>, where likewise no excited O atoms were to be found.

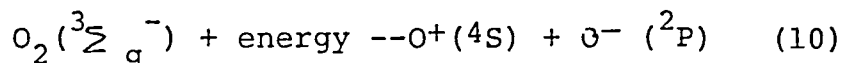
The formation of oxygen atoms in the procedure described here results within the given limits only in particles in the basic state. Thereby two significant source of distortion of the measurement of the O ionization cross section are eliminated. Further sources of distortion are dissociative ionization from  $H_2O$  and  $O_2$ , that lead to the population of mass 16.



Whereas  $O^+$  ions are not to be found in (7),  $O^-$  ions are found in measureable concentrations in (8). For this reason, the effective cross section of  $O^+$  formation  $\sigma(O^+, O_2)$  was measured using (8). Fig. 4 shows the energy declivity of the effective cross section according to (8), for the light source emission lines utilized in measuring the photoionization of the oxygen atom. The measureable ion beam has a wavelength range between 660 and 644 Å. This energy corresponds to the process



The calculated threshold energy for this ionization process is 18.72 eV ( $\approx 662\text{\AA}$ )<sup>11</sup>. Electron collision values for the process (9) are 19.2 and 18.9 eV  $\pm$  0.2 eV respectively.<sup>8, 12, 13</sup> Through the dissociation of the O<sub>2</sub> molecule into a negative and a positive ion, O<sup>+</sup> also results, according to equation (10)



The authors here show values between 16.9 and 17.2 eV. The calculated value lies at 17.27 eV ( $\approx 718 \text{\AA}$ ). Although an absorption of light, that according to (10) should lead to dissociation, constitutes an optically permissible transition, no O<sup>+</sup> ion current is found for these quanta energies. The effective cross section must, therefore, be quite small. The measured ion current for the line 660 Å equals zero within the failure limits shown in Fig. 4. This signifies that in this experiment no O<sup>+</sup> formation was noted for the energy 18.77 eV.

After consideration of the O<sup>+</sup> formation through dissociative ionization of the oxygen molecule, it is possible to calculate the values of ionization cross section of the oxygen atom shown in Fig. 5. The values shown are average values from ten independent measurements. The error of the effective cross section for a certain wavelength shown in Fig. 5 is composed of the error of relative and absolute measurement, and that of the absolute scale adjustment. The error of the relative effective cross section  $\sigma(\text{O}^+, \text{O})$  is, for certain favorable wavelengths, no greater than 3%, but on the average 7%. In addition to the errors in relative values, the total error of the absolute values also contains the pressure measurement error in the ionization chamber, the photoelectric yield error, the error in determination of degree of dissociation and ion current relationship, as well as the error from the adjustment of relative values to an absolute determination. From these factors, an average quadratic error of 10% is estimable for the values in Fig. 5.

FIG. 4. Effective cross section for  $O^-$  formation by dissociative ionization.

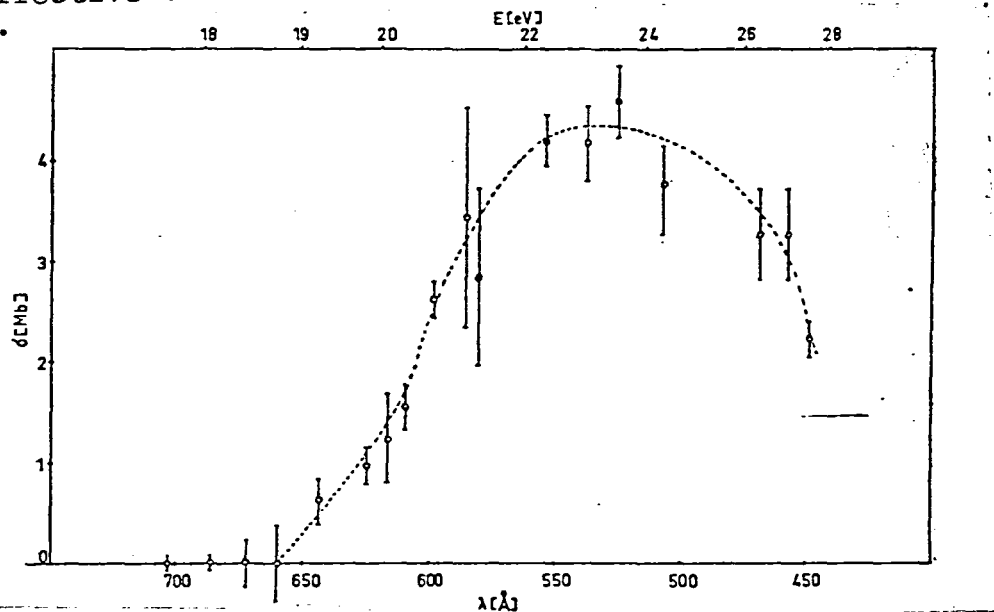
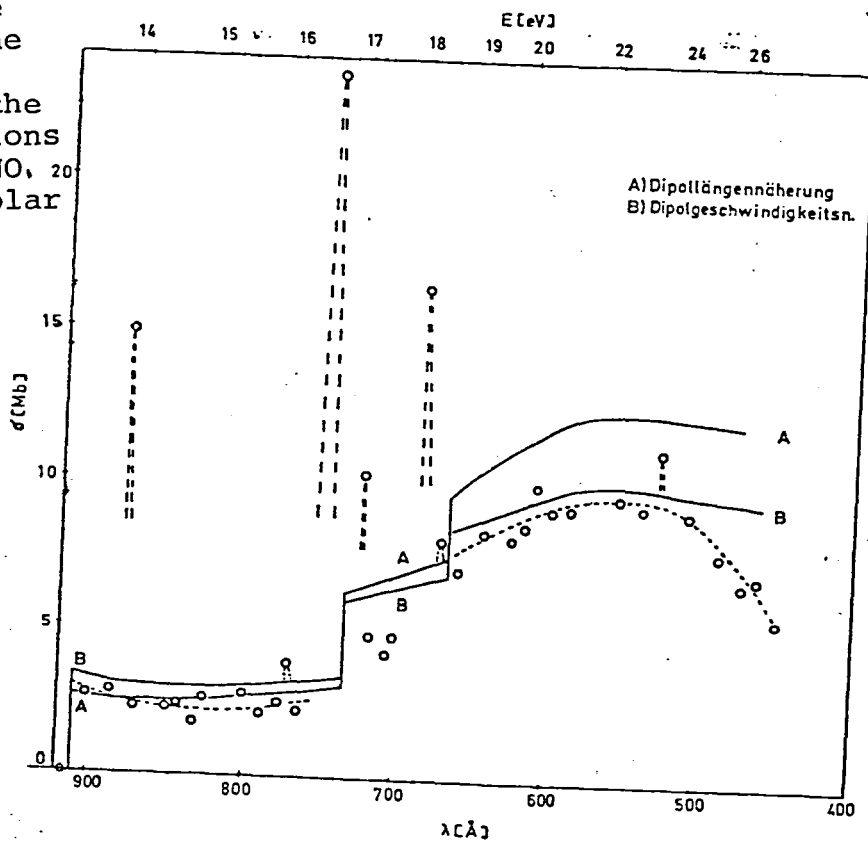


FIG. 5. Effective cross section for the photoionization of the oxygen atom in basic state. See further the effective cross sections calculated by DALGARNO, 20 and coworkers.<sup>5</sup> (Dipolar length/dipolar speed formula).



## DISCUSSION OF THE MEASUREMENT RESULTS/FINDINGS

The effective cross section of the photoionization of the oxygen atom depicted in Fig. 5 shows not only the measured points, but also a median curve, that at best connects the measured points to each other. In the range of median energies, this curve was not drawn in. Values falling sharply outside of the median curve are to be considered as maxima. Further, two results of calculations of the effective cross section by DALGARNO, HENRY and STEWART, are shown.<sup>5</sup> Curve A was calculated according to the dipole-length approximation, Curve B according to the dipole-speed approximation. The calculations represent only the cross section effected by direct transitions into the ionization continuum. Transitions to quasistationary states above the ionization boundary were not considered. These latter transitions, that in the case of the oxygen atom for the most part lead to autoionization, occasion a strong structure of the effective cross section. Since these measurements were carried out against the background of a line spectrum, the full structure is only observable in the case of the energy of an emission line of the light source coinciding with that of an autoionizing state. Should these autoionizing states be very wide, as is the case with the noble gases in the range of  $^2P_{3/2}$  and  $^2P_{1/2}$ , then the chance of such a coincidence is great. Should the lines however be narrow resultant to their long lifespan, one would only seldom find such a coincidence. However, in the latter case, the autoionizing states of a Rydberg series can be considered an isolated terminus: the continuum between them is only little or not at all disturbed by autoionization. One can in this case expect that in an experimental structure such as this one, maxima, and if circumstances dictate, minima, of the ionization cross section will only seldom be registered, and that for the most part, will either provide the effective cross section of the undisturbed continuum, or the values for the autoionization in the sphere of the resonance.

The latest calculations of the absorption behavior of atomic oxygen however shows that the autoionizing termini of the oxygen atom are in the range of the ( $^4S^{\circ}$ )- and ( $^2D^{\circ}$ )-

states of the  $O^+$  ion and are not very broadened.<sup>14</sup> ((The symbol  $^{\circ}$  indicates odd (uneven) parity throughout this paper)). This means that precisely the described phenomenon of quasiisolated termini appears. Thus, they substantially represent the ionization continuum calculated by DALGARNO and coworkers.<sup>5</sup> One can then conclude, by comparing measurements and theory, that both coincide within the margin of error. The median value of the effective cross section lies, however, somewhat lower than the theoretical curve calculated according to the dipole length approximation.

The oxygen ion has a  $(1s)^2 (2s)^2 (2p)^3$  configuration. The states  $^4S^{\circ}_{3/2}$ ,  $^2D^{\circ}_{5/2,3/2}$ , and  $^2P^{\circ}_{3/2,1/2}$ . Nine optically allowed series converge onto these lowest ionization states of the oxygen atom:

$$1) \quad 2p^3(^4S^{\circ}) ns^{\circ} ^3S^{\circ}, \quad (11) \quad (11)$$

$$2p^3(^4S^{\circ}) nd^{\circ} ^3D^{\circ}. \quad (12) \quad (12)$$

(11) and (12) are without interest for the discussion of ionization cross sections, since the termini lie below the lowest ionization border

$$2) \quad 2p^3(^2D^{\circ}) ns' ^3D^{\circ}, \quad (13) \quad (13)$$

$$2p^3(^2D^{\circ}) nd' \begin{cases} ^3S^{\circ}, \\ ^3P^{\circ}, \\ ^3D^{\circ}. \end{cases} \quad (14a-c) \quad (14a-c)$$

Of these series, the transitions from  $^3P^U$  (14b) are not allowed by the rules of autoionization. These are therefore observed in the emission. Lines of autoionizing series are slightly diffuse.

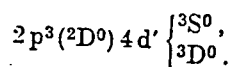
$$3) \quad 2p^3(^2P^{\circ}) ns'' ^3P^{\circ}, \quad (15) \quad (15)$$

$$2p^3(^2P^{\circ}) nd'' \begin{cases} ^3P^{\circ}, \\ ^3D^{\circ}. \end{cases} \quad (16a, b) \quad (16a-b)$$

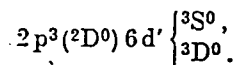
Whereas the termini of (15) and (16a) can only decay in the continuum to  $nd'^3P^{\circ}$ , an autoionization of the termini in (16b) is possible in several continua.

An investigation of the measured points in Fig. 5 in the  $^4S^{\circ}$  continuum shows that for the positions 879, 772, and 747 Å, the measured points diverge from the median curve substantially. The emission lines of the light source are in most cases groups of

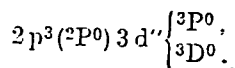
lines, and the indicated wavelengths represent only the concentration of these line groupings. No optically allowed transitions can be excited through absorption of the line at 879 A, whose decay into the  $4S^0$  continuum through autoionization is allowable by the rules of selection.<sup>15</sup> However, absorption into the  $2p^3 ({}^2P^0) 3s'' {}^3P^0$  state is optically allowable, since this state energetically correlates to the position of an emission line. Because of the demand to sustain the rotary impulse, this state can not decay into the lowest ionization continuum. The following transitions with subsequent autoionization into the  $4S^0$  continuum are possible for the absorption of the wavelength at 772 A:



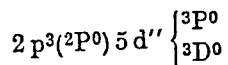
Likewise, for the absorption of the line at 747 A:



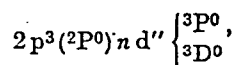
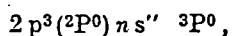
In the range of the second ionization continuum  $2D^0$  are three measured points that are also significantly higher than usual, namely those at 724, 686, and 672 A. Absorption termini with permissible transitions into the ionization continuum are available for all three lines. The following transitions exist to interpret the measured values at wavelength 724 A:



For absorption at wavelength 686 A the transitions:



and for that at 672 A the transitions:



where  $n=9, 10, 11$ . The indicated peak value at wavelength 526 A has no particular O atomic state, since the locus of the termini below 665 A is not known.

No median effective cross section was indicated in Fig. 5 between 731 and 665 A.

No transitions exist for the three lowest measured points that can lead to autoionization.



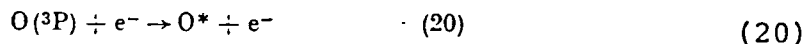
It is to be expected that the locus of these points corresponds to the locus of the  $2D^0$  continuum. A divergence of these points from the value for continual absorption would be possible, if a clear broadening of the autoionization termini were present in this area. Such an effect manifests itself for the autoionizing lines in this wavelength range.<sup>14</sup> Despite this, it can be assumed that the effective cross section in the range of the  $2P^0$  continuum will be lower than that calculated by DALGARNO and coworkers.<sup>5</sup> The measured points above the  $2D^0$  state of the  $O^+$  ion correspond well to those calculated by DALGARNO according to the dipole speed approximation formula up to 550 Å. However, below 550 Å, the measured effective cross section falls rapidly with a shrinking wavelength. Those values calculated with the dipole speed approximation are also considered probably better by the authors.

Since oxygen is the most important component of the upper ionosphere, its effective cross section is of great significance in calculating charged particle density and particle temperature. Measurements of radar returns have shown that during the day at altitudes higher than 300 km, the temperature of positive ions is higher than that of neutral particles.<sup>16</sup> These conclusions agree with theoretical prognoses, when one assumes the heating of ionic components through elastic collisions with hot electrons and their cooling off through elastic and unelastic collisions with neutral particles.<sup>17, 18</sup> Since the electrons resultant to photoionization are the primary energy carriers, knowledge of their primary energy distribution is of special interest. This distribution can, however, be estimated from the spectrum of ionizing radiation and the effective cross section of those particles that attain ionization.

Absorption from the basic state of the atom is of especial significance for the photoionization of the O atom in the upper ionosphere:



One must also, however, consider exciting electron collisions, that lead to the formation of excited atoms. O can be a  $^1D$  state here.



As SAGALYN and coworkers have found, high values show up in the electron temperature for a short time after sunrise in an altitude of 250 km.<sup>19</sup> A cooling off of the electrons through collisions with neutral oxygen atoms becomes important.<sup>20</sup> The emission of red oxygen lines from the disallowed  $^1D-^3P$  transition were observed simultaneously with the high value electron temperature. The high temperatures of the electron gas are only present for a short time after sunrise, so the probability for the process (20) becomes rapidly smaller.

Since the O ionization cross section was measured with a line spectrum, a comparison of the solar spectrum with that of the light source is interesting. The intensity of the light source spectrum is quite high in the lower energy range of the oxygen ionization continuum, and doesn't drop to 1/10 of the value until it falls below 680 A. Between 800 and 910 A, the solar spectrum shows a relatively intense emission continuum, that is covered with strong oxygen lines at 834 A.<sup>20, 21</sup> These oxygen lines are strongly emitted by the light source. Furthermore, down to 450 A, a row of oxygen and nitrogen lines appear in the solar spectrum, that are all present in the light source spectrum, since this is advantageously composed of the familiar oxygen, nitrogen and argon lines. This however signifies that the effective cross section of the oxygen atom measured with the line light source can be utilized directly for the calculation of the ionizing effect of solar radiation. Below 630 A, one finds several strong helium, neon, magnesium, and silicium lines as well in the solar spectrum. However, in this range the measured effective cross section is almost without structure, so that one can interpolate quite well between the measured points. The aforementioned sunlight continuum between 910 and

800 A is of especial significance to the ionization of the oxygen atom. Here, a number of autoionization processes give the ionization cross section a strong structure. The measured effective cross section for the autoionization in the  $4S^0$  continuum can assume the tenfold value of the undisturbed ionization continuum, as the measured point for the wavelength 747 A shows. It is however not certain whether this recorded measured value corresponds to the maximum of the autoionizing termini grouping. One can probably assume that the absorption in the range of the autoionizing termini is significantly higher. Even if the coincidence of an oxygen terminus and one of the lines in the line packet at 747 A should be exact, its intensity is only a small fraction of the intensity of the entire line grouping considered for the calculation of the effective cross section. The autoionizing termini of the oxygen atom are of lesser significance for the solar radiation-occasioned oxygen ionization below 800 A, since there is only a marginal coincidence between the emission lines of the solar spectrum and the autoionizing termini of oxygen in this wavelength range. There is possibly such a coincidence present at 770 A. With the aid of an intensity specification of the solar spectrum, and the measured effective cross section of the oxygen atom, it is possible to estimate the extent of the oxygen ionization. This shall, however, not occur within the framework of this study, and shall be deferred to a later time, once the measuring of the ionization cross section with the background of a continuum has been accomplished. Such a measurement will result in a more precise estimation of the contribution of the autoionizing termini to the ionization of the oxygen atom.

We thank the German Research Society for its support of this study.

## LITERATURE

1. F.J. Comes and U. Wenning, Phys. Lett. 23, 537 [1966].
2. F.J. Comes, A. Elzer and F. Speier, Z. Naturforsch. 23a, 114 [1968] this project.
3. D.R. Bates and M.J. Seaton, Mon. Not. Roy. Astr. Soc., 109, 698 [1949].
4. A. Dalgarno and D. Parkinson, J. Atmos. Terr. Phys. 18, 335 [1960].
5. A. Dalgarno, R.J.W. Henry, and A.L. Stewart, Planet.Space Sci. 12, 235 [1964].
6. R.B. Cairns and J.A.R. Samson, Phys. Rev. 139A 1403 [1965].
7. F. Kaufman and J.R. Kelso, J. Chem. Phys. 32, 301 [1960].
8. J.T. Herron and H.I. Schiff, Can. J. Chem. 36, 1159 [1958].
9. R.A. Young, Private Report; - R.A. Young and G. Black, J. Chem. Phys. 44, 3741 [1966].
10. W.L. Fite and R.T. Brackmann, Phys Rev. 113, 815 [1959].
11. F.R. Gilmore, J. Quant. Spectrosc. Radiat. Transfer. 5 369 [1965].
12. R. Thorburn, Applied Mass Spectrometry, The Institute of Petroleum, London, 1955, p. 185.
13. H.D. Hugstrum, Rev. Mod. Phys. 23, 185 [1951].
14. R.E. Huffman, J.C. Larrabee, and Y. Tanaka, J. Chem. Phys., 46, 2213 [1917].
15. G. Herzberg, Atomic Spectra and Atomic Structure, Dover Publications, New York, 1944.
16. J.V. Evans, Planet. Space Sci., 13,1031 [1965].
17. A. Dalgarno and I.C.G. Walker, Planet. Space Sci. 15, 331 [1967].
18. A. Dalgarno, M.B. McElroy, and I.C.G. Walker, Planet. Space Sci. 15, 331 [1967].
19. R.C. Sagalyn, M. Smiddy, and Y.N. Bhargava, Space Research V., ed. King-Hele, Muller, Righini, North-Holland Publishing Co. Amsterdam 1965.
20. L.A. Hall, K.R. Damon and H.E. Hinteregger, Space Research III., ed. Priester, North-Holland Publ. Co. Amsterdam 1963.
21. H.E. Hinteregger, L.A. Hall, and G. Schmidtke, Space Research V., ed. King-Hele, Muller, Righini, North-Holland Publ. Co., Amsterdam 1965.

**End of Document**